JCTC Journal of Chemical Theory and Computation

Impact of PES on MD Results of the Coalescence of M_2 + M with M = Ir, Pt, Au, Ag

Tiffany Pawluk, Li Xiao, Jennifer Yukna, and Lichang Wang*

Department of Chemistry and Biochemistry, Southern Illinois University, Carbondale, Illinois 62901

Received August 8, 2006

Abstract: The accuracy of the Sutton−Chen potential energy surface (PES) for describing atomic interactions in small metal clusters was investigated by comparison with density functional theory (DFT) calculation results. The binding energies calculated using the Sutton−Chen PES for the dimers, trimers, and 8- and 13-atom clusters of four transition metals, Ir, Pt, Au, and Ag, differ from those obtained with DFT calculations. As the DFT results agree well with the available experimental data, the above disagreement indicates that the original Sutton−Chen PES cannot accurately describe the interactions among atoms in the cluster for these metals. The parameters of the Sutton−Chen potential were therefore optimized to the DFT results for each of the metals. Molecular dynamics (MD) simulations were carried out on the coalescence of a dimer with a single atom for these metals. Both the original bulk and the cluster optimized Sutton−Chen PESs were tested with various incident angles and initial kinetic energies. The MD results show that the coalescence is highly dependent on the PES. This demonstrates that use of an accurate PES is critical, particularly at low-energy regime. The kinetic energy, incident angle, and choice of metal were examined for their role in the outcome of the coalescence process.

1. Introduction

Many fascinating properties exhibited by nanomaterials are highly size dependent.[1−3] For example, it is well-known that bulk gold is an inert material. However, temperature-programmed reaction studies revealed that small Au clusters with less than 20 atoms are active for CO combustion, and the catalytic activity varies with cluster size.[4] Small clusters are highly active and may aggregate if they are placed close to each other under suitable conditions.[1,5,6] This formation of large particles due to the aggregation of small clusters, often termed sintering in catalysis, is largely responsible for the complete loss of catalytic activities.[7−24] Despite this consequence, no effective control over this process has been possible due to a lack of understanding of the coalescence or association processes. It is therefore important to understand the coalescence mechanism.

Computationally, Monte Carlo (MC) and molecular dynamics (MD) methods are two common choices used to study the coalescence of large size metal clusters. For example, Tian and Guo performed MC simulations using the Lennard-Jones plus Axilrod-Teller potential to study the growth of 13- and 39-atom clusters for Ag, Au, Ni, and Pd metals.[25] Another example is the use of MD simulations by Hendy et al. to study the coalescence of Pb clusters.[26]

In either MC or MD simulations, a potential energy surface (PES) is used to describe the interactions among atoms in the system. There are four types of PESs, i.e., the Finnis−Sinclair potentials,[27] the embedded atom potentials,[28] the tight binding potentials,[29] and the Murrell−Mottram potentials,[30] which have been widely used for describing interactions among transition metal atoms. These potentials all incorporate parameters fitted to bulk or solution metals. Our goal is to test the reliability of each of these potentials for modeling small metal clusters. We begin our investigation with the Sutton−Chen potential,[31] which is a modified Finnis−Sinclair potential. It seems to be suitable for studying coalescence of transition metal clusters, as it is a many-body

* Corresponding author phone: (618)453-6476; fax: (618)453-6408; e-mail: lwang@chem.siu.edu.

10.1021/ct600257p CCC: $37.00
Published on Web 01/05/2007

Table 1. Original Sutton−Chen (Bulk) Potential Parameters[a] and Optimized (Cluster) Potential Parameters for Ir, Pt, Au, and Ag[b]

			ϵ (eV)		c		α (Å)	
	m	n	bulk	cluster	bulk	cluster	bulk	cluster
Ir	6	14	0.0024489	0.0025500	334.94	328.22	3.84	3.45
Pt	8	10	0.019833	0.011306	34.408	33.851	3.92	3.90
Au	8	10	0.012793	0.0064582	34.408	33.857	4.08	4.08
Ag	6	12	0.0025415	0.0018828	144.41	144.36	4.09	4.04

[a] See ref 31. [b] The parameters m and n were kept the same, while ϵ, c, and a were optimized.

potential and has been used to search for the global minimum of transition metal clusters.[32]

The parameters used in the Sutton−Chen potential were optimized by fitting to the bulk properties of each metal. Therefore, before carrying out MD simulations of coalescence for transition metal clusters, it is necessary to investigate whether the Sutton−Chen potential can be used to accurately describe the interactions among transition metal atoms in small systems. As the extensive results obtained for transition metal clusters from density functional theory (DFT) calculations[33−36] have just become available, it is possible to investigate the accuracy of the PESs.

The purpose of this current work is twofold. First, we investigated whether the Sutton−Chen potential is accurate for describing the interactions among atoms in a particle. We chose four metals, i.e., Ir, Pt, Au, and Ag, as our systems in this work. We calculated the binding energies for a number of clusters using the Sutton−Chen potential, and compared these results with the DFT results for those metal clusters. As our comparison has shown, the original bulk PES was not accurate; we therefore obtained cluster optimized parameters for the Sutton−Chen potential. Second, we performed MD simulations using the Sutton−Chen potential with both original bulk and cluster parameters in order to investigate the impact of different PESs on the outcome of a coalescence process. The MD simulations were performed to study the reaction dynamics of a single metal atom colliding with a metal dimer, i.e., A + BC with A=B=C = Ir, Pt, Au, or Ag. As those metal atoms are heavy compared to others such as the hydrogen atom, we expect that the quantum effect is negligible in the reaction dynamics. Therefore, we chose to use classical trajectory calculations in our study. Furthermore, the current MD studies focus on comparing individual trajectories at different incident angles and kinetic energies as well as on investigating how the choice of metal affects the outcome of an individual trajectory of the same given conditions. Throughout this work, special attention was given to the impact of PES on the outcome of the MD simulations in an effort to develop a better understanding of the critical role of the PES.

2. Simulation Details

In MD simulations, whether a full quantum or a classical treatment is employed, the PES is the most important part if accurate results are to be obtained. As such, we will discuss the PESs that were used in our simulations first and then provide the details of the MD simulations.

2.1. Potential Energy Surface (PES). In the MD simulations, we used the Sutton−Chen potential[31]

$$V = \epsilon\left[\frac{1}{2}\sum_{ij} v(r_{ij}) - c\sum_{i}\sqrt{\rho_i}\right] \tag{1}$$

where the pair potential is given by

$$v(r_{ij}) = \left(\frac{a}{r_{ij}}\right)^n \tag{2}$$

and the local electron density is given by

$$\rho_i = \sum_j \left(\frac{a}{r_{ij}}\right)^m \tag{3}$$

to describe the interactions among atoms in the system. In eqs 1−3, r_{ij} is the distance between two atoms, and ϵ, a, c, m, and n are parameters, which are constant for each metal but vary for different metals. These potential parameters were obtained by Sutton and Chen[31] for different metals by fitting the bulk properties of each metal. The Sutton−Chen parameters for iridium, platinum, gold, and silver are summarized in Table 1.

Our comparison of binding energies obtained using the Sutton−Chen potential with the parameters originally provided by Sutton and Chen with the DFT results[33−36] for several clusters of Ir, Pt, Au, and Ag showed that it was necessary to improve upon the Sutton−Chen parameters for clusters of those metals. In this work, we therefore obtained cluster optimized parameters for each metal. The details of this are discussed in section 3.1.

2.2. Molecular Dynamics (MD) Simulations. We studied the coalescence of an atom and a dimer by solving the equations of motion for position

$$\frac{dx_i}{dt} = \frac{p_{x_i}}{m_i}, \frac{dy_i}{dt} = \frac{p_{y_i}}{m_i}, \frac{dz_i}{dt} = \frac{p_{z_i}}{m_i} \tag{4}$$

and momentum

$$\frac{dp_{x_i}}{dt} = -\frac{\partial V}{\partial x_i}, \frac{dp_{y_i}}{dt} = -\frac{\partial V}{\partial y_i}, \frac{dp_{z_i}}{dt} = -\frac{\partial V}{\partial z_i} \tag{5}$$

based on the Cartesian coordinates x, y, and z for each atom, i, with $i = 1-3$, where m_i is the mass of the ith atom, and V is the PES described in section 2.1. The above set of coupled equations was solved using the sixth-order Runge−Kutta method.[37] Although other coordinate systems, such as the Jacobi coordinates, can be used here, we adopted Cartesian coordinates. Our intention of building the dynamics code is for studying systems consisting of more than 100 metal atoms where the Cartesian coordinates are the most practical choice.

The coalescence was studied as a single atom approached a dimer, first collinearly, i.e., the incident angle, θ, is zero. A schematic illustration of the system is provided in Figure 1. The starting position of each atom was specified as follows. The bond distance of the dimer equals the equilibrium dimer distance for each metal. The equilibrium distance was obtained by calculating the binding energy of the dimer

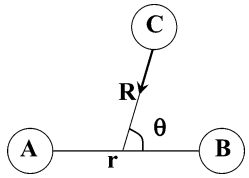

Figure 1. Schematic illustration of the system studied: a single metal atom C colliding with a metal dimer AB with A=B=C = Ir, Pt, Au, or Ag. *R*, *r*, and θ are in Jocobi coordinates. The arrow indicates the direction of the initial momentum of atom C.

as a function of distance using the Sutton−Chen potential. The initial distance between the center of mass of the dimer and the third atom was set to be 10 Å, a sufficient distance to ensure that the single atom and the dimer are in the asymptotic region. Initially, the dimer is in its ground rotational and vibrational states.

In order to study how the coalescence depends on kinetic energy, the initial kinetic energy provided to this collinear system was varied from 0.02 to 2.0 eV. The single atom has the entire kinetic energy, and the direction of its momentum is along the incident angle (see Figure 1). To investigate how the incident angle affects coalescence, the incident angle was varied by 15° from linear, $\theta = 0$, until the third atom was approaching the dimer from a perpendicular direction, $\theta = 90°$. Energies of 0.1 and 1.0 eV were tested for each of the different incident angles.

The positions and momentum of atoms were calculated at each time step of 0.01 fs for 10 ps or until the distance between any two atoms exceeded 10 Å. The products from most trajectories using the above stopping criterion are a dimer and an atom instead of trimer complexes, as will be shown in section 3.2. This indicates that the reaction time is less than 10 ps for the majority of the systems being studied. Furthermore, the focus of the current work is to investigate the impact of different PESs on the outcome of single coalescence processes. The choice of 10 ps is sufficient.

For testing our assumptions to be discussed in section 3.2, we ran some trajectories long enough so that the complex trimers dissociate. During the entirety of the simulations, the total energy and the total linear momentum of the system were conserved.

These MD simulations were carried out using the original Sutton−Chen parameters and again with the improved parameters. The final products were analyzed, and the results are discussed in section 3.2. The vibrational state of the product dimer, where present, was estimated using a harmonic oscillator treatment, in which the vibrational state, v, was calculated by

$$E_{\text{dimer}} = h\omega_e\left(v + \frac{1}{2}\right) \tag{6}$$

where h is the Planck's constant, $\omega_e = 1/2\pi\sqrt{k/\mu}$ with μ being the reduced mass of the product dimer and k being the force constant obtained from the dimer potential curve, and E_{dimer} is the vibrational energy of the product dimer. We note that at high vibrational states, the result will be approximate.

Table 2. Comparison of Binding Energy Obtained Using the Original Bulk and Cluster Optimized Parameters of Sutton−Chen Potential and DFT Calculations[a]

		binding energy (eV)			
		original PES	cluster PES	DFT and references	
Ir	dimer	−2.73	−5.06	−5.06	
	linear trimer	−0.15	−8.09	−9.63	ref 33
	triangle	−8.56	−9.46	−9.09	
Pt	dimer	−7.29	−4.03	−3.52	
	linear trimer	−11.41	−6.32	−6.54	ref 34
	triangle	−12.28	−6.79	−6.99	
Au	dimer	−4.46	−2.20	−2.34	
	linear trimer	−6.91	−3.42	−3.57	ref 35
	triangle	−7.43	−3.67	−3.57	
Ag	dimer	−2.29	−1.68	−1.80	
	linear trimer	−3.73	−2.73	−2.64	ref 36
	triangle	−3.85	−2.74	−2.64	

[a] The reference point of the energy is the asymptotic region of isolated atoms.

3. Results

The results of our study of the potential energy surfaces are presented in section 3.1. The molecular dynamics simulation results are presented and discussed in section 3.2.

3.1. New Parameters for the Sutton−Chen PESs. The quality of the PES is one of the most important factors in determining the accuracy of the results obtained from MD simulations, so we began our investigation here. Using the parameters published by Sutton and Chen,[31] we calculated the PES for each of the metals iridium, platinum, gold, and silver. Throughout this paper, we refer to this PES as the "original bulk PES" using the "original bulk parameters". Using this original PES, we calculated the binding energy of a dimer, linear trimer, triangular trimer, and 8- and 13-atom cluster for each of the metals and compared the results with our previous DFT findings for the binding energy of these clusters. The geometries chosen were the relaxed structures obtained by DFT. The DFT data used has been proven reliable compared to experimental and other theoretical methods through our previous work.[33−36] For example, the DFT binding energy of Ir_2, Pt_2, Au_2, and Ag_2 is −5.06 eV,[33] −3.52 eV,[34] −2.34 eV,[35] and −1.80 eV,[36] respectively, which agrees well with the experimental values, −4.30 eV for Ir_2,[38] −3.14 eV[39] and −3.66 eV[40] for Pt_2, −2.29 eV for Au_2,[41] and −1.65 eV for Ag_2.[42] In contrast, the original bulk Sutton−Chen potential gives a drastically different binding energy of −2.73 eV, −7.29 eV, −4.46 eV, and −2.29 eV for Ir_2, Pt_2, Au_2, and Ag_2, respectively. The huge discrepancy in the dimer binding energy between the experiment/DFT and the Sutton−Chen potential is not surprising, as the original Sutton−Chen potential was only fitted to the bulk properties.

The results of the binding energies from the original Sutton−Chen PES and the DFT calculations for the dimer, linear trimer, and triangular trimer are summarized in Table 2, as they are more relevant to the current work. The conclusions from the comparison on the 8- and 13-atom clusters of these four metals are similar to those on the dimer and trimers. As shown in Table 2, the binding energies calculated from the original PES are considerably different

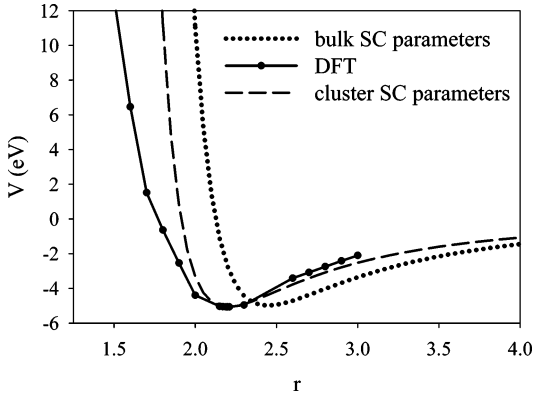

Figure 2. Comparison of the potential energy, *V* (in eV), vs the bond distance, *r* (in Å), for iridium dimers calculated with the original bulk and cluster optimized Sutton−Chen potentials and DFT.

from the DFT results. We use the binding energy as a measure of the stability of the clusters. As it is defined for these calculations, a lower binding energy indicates a more stable structure. Of greater importance is that the relative stability of the trimers does not correspond to the DFT predictions. For iridium, the binding energy predicted by DFT calculations is −9.63 eV for the linear trimer and −9.09 eV for the triangle. However, the binding energies calculated from the original PES are −0.15 eV and −8.56 eV for the linear trimer and triangle, respectively. This indicates the opposite order of stability. Discrepancies are also apparent for the other metals. The binding energies for platinum and gold are about 2 times lower than the DFT values, and the results for silver are similarly problematic.

It was necessary to improve upon the original parameters for these small metal clusters. In our fitting, we fixed *m* and *n* but optimized ϵ, *a*, and *c* so that the binding energies using the optimized parameters are close to the DFT results. Such a choice is somewhat arbitrary, but the optimized results show that the choice is reasonable. For the purpose of this work, we did not choose to use other fitting strategies. In the ongoing research efforts to fit the Sutton−Chen potential including large clusters, we will examine different strategies, such as allowing the parameters *m* and *n* to be optimized as well.

A nonlinear least-squares fitting procedure was used.[33] The parameters were optimized by fitting the DFT results for the dimers at various bond distances and two trimers, linear and triangular, for each metal, as it is directly relevant to the current work. Several sets of parameters were acceptable for each metal, but the optimal parameters are included in Table 1. These cluster optimized parameters were used to construct a new PES for each metal. We will refer to this case throughout this paper as the "cluster optimized PES" and "cluster optimized parameters". The binding energies were calculated for the DFT structure for the dimer at equilibrium distance, and two trimers using this cluster optimized PES. These results for the binding energies are also included in Table 2.

Figure 2 shows the potential curves as a function of dimer bond distance for the iridium dimer calculated by both the bulk and cluster potentials as well as DFT. The original potential gives a reasonable estimate of the global minimum energy for the dimer, at −4.99 eV, but gives very poor agreement with the equilibrium bond distance of 2.45 Å. The DFT results are −5.06 eV and 2.19 Å, respectively. This bulk potential yields a binding energy of −2.73 eV for the DFT structure, which is very different from the DFT binding energy. The cluster optimized potential provides excellent agreement with the DFT results in the minimum region of the curve. We emphasize this region from 2 to 3 Å because the DFT calculations are most reliable here. At bond distances less than 2 Å and longer than 3 Å, i.e. shorter and longer distances, the DFT results are less reliable. The details of the DFT work can be found in refs 33−36.

The new parameters provide very good agreement between the Sutton−Chen potential and DFT results for trimers and similar variations for the 3-atom isomers for each metal. The binding energies from the cluster optimized Sutton−Chen potential for all the metals are much closer to the energies obtained by DFT for all structures.

The binding energies reported in Table 2 were calculated for the DFT geometries. Our comparison of the global minima from the cluster Sutton−Chen potential with these fixed geometry results shows good agreement. For example, the binding energy for the iridium dimer exactly corresponds to the global minimum, and the trimer results agree within 0.3 eV. The equilibrium bond distances of 2.20 Å and 2.31 Å agree within 0.06 Å to the DFT values of 2.16 Å and 2.37 Å for the linear trimer and triangle, respectively. The global minima from the original Sutton−Chen potential occur at an overestimated bond distance of 2.50 Å and 2.53 Å for the linear and trianglar trimer, respectively.

The original and cluster optimized PESs were obtained and compared for each metal for the collinear interaction of three atoms, A, B, and C. As an example, the cluster and bulk PESs for iridium are shown in Figure 3. The potential energy in eV is plotted as a function of the AB distance and BC distance in Å. Overall topology of the PES remains the same. However, as illustrated by the MD simulations to be discussed below, the two PESs produce rather different results.

3.2. Coalescence of AB + C with A=B=C = Ir, Pt, Au, and Ag. We studied the coalescence of a 3-atom system for iridium, platinum, gold, and silver using MD simulations. The initial state of the 3-atom system was a single atom C colliding with a dimer AB at its ground rovibrational state (Figure 1). The MD simulations were performed using the original bulk and cluster optimized PESs described above. A total of 176 trajectories were obtained, and the products are summarized in Tables 3−5. The products from 80% of the total trajectories are a dimer and an atom, and they were formed long before the 10 ps maximum simulation time was reached. In addition to the dimer and atom as the major products, 34 triatomic complexes were still formed at the end of the simulation, i.e. 10 ps. Because the total energy of the system is conserved, these triatomic complexes formed during the coalescence may dissociate into an atom and a dimer if the MD simulation is run for more than 10 ps. To illustrate the possible dissociation of the triatomic complex still being formed at 10 ps, we carried out the MD simulation

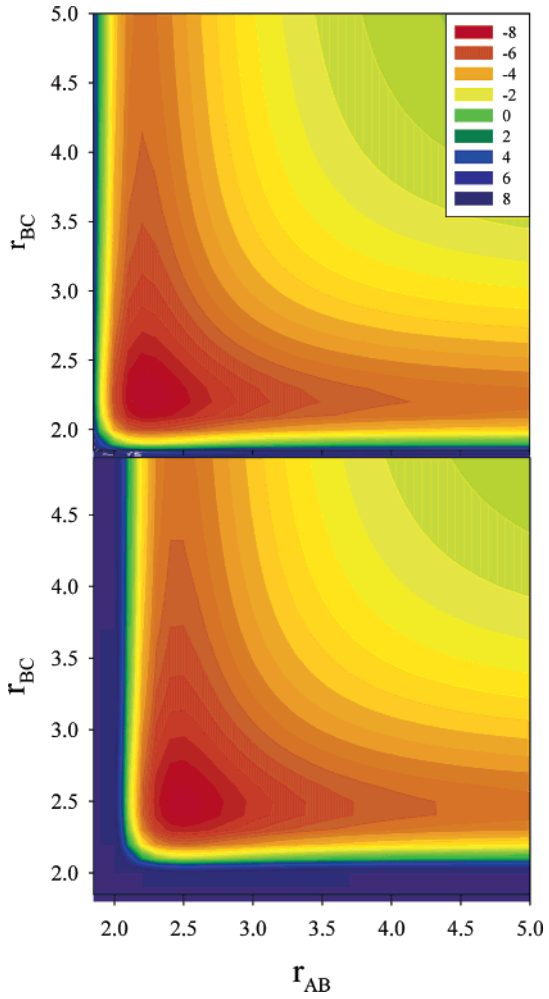

Figure 3. The cluster optimized (top) and original bulk (bottom) Sutton−Chen PES for the collinear AB + C reaction of Ir atoms. The legend shows the potential energy in eV. The interatomic distances, r_{AB} and r_{BC}, are given in angstroms (Å).

for the Ag_2 + Ag system with an initial kinetic energy of 0.1 eV and an incident angle of 45° for longer than 10 ps. The results show that an Ag triatomic complex was formed during the coalescence, and it remained as a complex at 10 ps. At 65.8 ps, the Ag triatomic complex dissociated into Ag_2 + Ag. The formation rate of triatomic complexes, the lifetime of the nascent triatomic complexes, and the energy transfer during a coalescence process are important and interesting issues that need to be addressed in order to fully understand the coalescence processes. Research in this direction is in progress. The work in progress also includes exploring the ways of extracting excess energy from the system so that real sintering processes can be simulated.

In order to investigate how the kinetic energy affects the coalescence of the AB + C system, the initial kinetic energy was varied from 0.02 to 2.0 eV, while the incident angle was kept at 0°. The results are summarized in Table 3. We first discuss the impact of the PES on the results of the collinear reaction dynamics. At lower energies, i.e., the kinetic energy less than 0.2 eV, the cluster PES resulted in more cases of elastic scattering for the lower energies of 0.02, 0.05, and 0.1 eV, as shown by the data in Table 3. In the energy range of 0.2−0.5 eV, the dynamics outcome for

Table 3. Final Product(s) for the Collinear AB + C Reaction as a Function of Initial Kinetic Energy, E_T, for Iridium (Black), Platinum (Red), Gold (Blue), and Silver (Green)[a]

E_T (eV)	Bulk Sutton-Chen parameters			Cluster Sutton-Chen parameters		
	AB+C	A+BC	A-B-C	AB+C	A+BC	A-B-C
0.02		Ir (v=0) Ag (v=0)	Pt (A-B-C) Au (A-B…C)*	Pt (v=0)	Ir (v=2) Ag (v=0)	Au (A-B-C)
0.05	Pt (v=0) Au (v=0)	Ir (v=0) Ag (v=0)		Pt (v=0) Ag (v=0)	Ir (v=1) Au (v=1)	
0.1	Pt (v=0) Au (v=0)	Ir (v=1) Ag (v=1)		Pt (v=2) Ag (v=0)	Ir (v=0)	Au (A-B-C)
0.2	Au (v=0)	Ir (v=0) Pt (v=2) Ag (v=5)			Ir (v=1) Pt (v=1) Ag (v=1)	Au (A-B-C)
0.3		Ir (v=0) Pt (v=0) Ag (v=0)	Au (A-B-C)		Ir (v=0) Pt (v=0) Au (v=1) Ag (v=0)	
0.4		Ir (v=0) Ag (v=0)	Pt (A…B-C)* Au (A-B-C)	Pt (v=3) Au (v=0) Ag (v=0)	Ir (v=0)	
0.5	Pt (v=0)	Ir (v=0) Ag (v=0)	Au (A-B-C)		Ir (v=0) Pt (v=0) Au (v=10) Ag (v=1)	
1.0		Ir (v=0) Pt (v=4) Au (v=0) Ag (v=0)			Ir (v=0) Pt (v=1) Au (v=10) Ag (v=0)	
1.5		Ir (v=0) Pt (v=0) Au (v=2) Ag (v=0)			Ir (v=2) Pt (v=0) Au (v=5) Ag (v=2)	
2.0		Ir (v=3) Pt (v=18) Au (v=10) Ag (v=0)			Ir (v=0) Pt (v=7) Au (v=5) Ag (v=0)	

[a] These results were obtained using the original bulk Sutton−Chen potential parameters as well as the optimized cluster parameters. The final vibrational state is included in the parentheses for cases where a dimer is one of the products. *A...B indicates an interatomic distance greater than 3.0 Å, so that these atoms do not form a real bond but rather a van der Waals complex.

three metals except Ir shows dependence on the PES but to a lesser extent compared to the lower energy range discussed above. At energies higher than 1 eV, the same products were formed, although the final vibrational state is still sensitive to the PES used. This indicates that the difference in PES shows less impact at the higher energies. In conclusion, the results in Table 3 show that the PES is critical in determining the outcome of a coalescence process, particularly at low-energy regime.

We now analyze the impact of kinetic energy on the reaction dynamics of a dimer colliding collinearly with an atom based on the MD simulations. The discussion of results in Table 3 is confined to those obtained using the cluster optimized parameters. For Ir, reactive scattering occurs with the product A + BC in every case. For Pt, Au, and Ag, the results in Table 3 show more variation in the products with different initial energies. The products obtained most frequently for Pt are again A + BC and elastic scattering occurring primarily at the lower energies from 0.02 to 0.1 and 0.4 eV. As for Ag, the products are the same as Au at kinetic energies higher than 0.2 eV. At 0.05−0.2 eV, the Ag system behaves similarly to the Pt system. At 0.02 eV, a reactive scattering occurs with the products of A + BC.

Au forms a trimer more frequently than elastic scattering and more often than any of the other metals. No trimer was formed for Ir, Pt, or Ag. This indicates that energy needs to be dissipated from the reaction complex in order to form a trimer such as using Ar atoms to absorb the energy, which is often used in the formation of transition-metal clusters.[2]

For collinear dynamics at kinetic energies larger than 0.5 eV, the results in Table 3 show that the products of the

Table 4. Final Product(s) for the AB + C Reaction with 1.0 eV of Initial Kinetic Energy as a Function of Incident Angle, θ, for Iridium (Black), Platinum (Red), Gold (Blue), and Silver (Green)[a]

Angle(°)	Bulk Sutton-Chen parameters				Cluster Sutton-Chen parameters			
	AB+C	A+BC	AC+B	ABC[‡], A-B-C, A-C-B, B-A-C	AB+C	A+BC	AC+B	ABC[‡], A-B-C, A-C-B, B-A-C
0		Ir (v=0) Pt (v=4) Au (v=0) Ag (v=0)				Ir (v=0) Pt (v=1) Au (v=10) Ag (v=0)		
15	Pt (v=2)	Ir (v=0) Au (v=3) Ag (v=10)				Ir (v=0) Pt (v=1) Ag (v=7)	Au (v=11)	
30	Ir (v=7) Pt (v=0)	Ag (v=16)		Au (A…B-C)*	Pt (v=2)	Ir (v=13) Au (v=2) Ag (v=0)		
45	Au (v=6) Ag (v=0)	Pt (v=7)	Ir (v=21)		Ir (v=0) Pt (v=3) Au (v=6)		Ag (v=0)	
60	Ir (v=9) Ag (v=0)		Au (v=13)	Pt (B-A-C)	Ir (v=5) Ag (v=10)		Pt (v=9)	Au (A-B-C)
75	Ir (v=4) Au (v=7) Ag (v=0)		Pt (v=1)		Pt (v=3)		Ir (v=3) Au (v=23) Ag (v=6)	
90	Ir (v=7) Ag (v=0)		Pt (v=1) Au (v=2)			Ir (v=4) Pt (v=4) Ag (v=7)		Au (A-C-B)

[a] These results were obtained using the bulk Sutton−Chen potential parameters as well as the optimized cluster parameters. The final vibrational state is included for dimer products, when present. ABC indicates a trimer of triangle shape. *A...B indicates an interatomic distance greater than 3.0 Å, so that these atoms do not form a real bond but rather a van der Waals complex.

Table 5. Final Product(s) for the AB + C Reaction with 0.1 eV of Initial Kinetic Energy as a Function of Incident Angle, θ, for Iridium (Black), Platinum (Red), Gold (Blue), and Silver (Green)[a]

Angle(°)	Bulk Sutton-Chen parameters			Cluster Sutton-Chen parameters			
	AB+C	A+BC	ABC[‡], A-B-C, A-C-B, B-A-C	AB+C	A+BC	AC+B	ABC[‡], A-B-C, A-C-B, B-A-C
0	Ir (v=0) Pt (v=0) Au (v=0)	Ag (v=1)		Ir (v=0) Pt (v=2) Ag (v=0)			Au (A-B-C)
15	Ir (v=2) Au (v=0) Ag (v=0)		Pt (A-B-C)	Ir (v=0) Au (v=1)	Pt (v=1) Ag (v=0)		
30	Au (v=1) Ag (v=0)		Ir (A-B-C) Pt (B-A-C)		Pt (v=3) Ag (v=5)		Ir (B-A-C) Au (A-B-C)
45		Ag (v=0)	Ir (A-C…B)* Pt (A-B-C) Au (A-B-C)	Pt (v=1)	Au (v=1)		Ir (A-B-C) Ag (A…B-C)*
60	Ir (v=1)		Pt (B-A-C) Au (A-B…C)* Ag (ABC)	Pt (v=1)	Ir (v=1) Ag (v=1)		Au (A-C-B)
75		Ag (v=0)	Ir (B-A-C) Pt (A-B-C) Au (A-B…C)*	Ag (v=0)	Pt (v=2)	Ir (v=2)	Au (ABC)
90	Ir (v=31) Pt (v=0) Ag (v=11)		Au (A…B-C)*	Pt (v=1) Ag (v=0)	Ir (v=6)		Au (A-B-C)

[a] These results were obtained using the bulk Sutton−Chen potential parameters as well as the optimized cluster parameters. The final vibrational state is included for dimer products, when present. ABC indicates a trimer of triangle shape. *A...B indicates an interatomic distance greater than 3.0 Å, so that these atoms do not form a real bond but rather a van der Waals complex.

dynamics are not sensitive to the type of metals. This indicates that the details of PESs are less critical at this energy range. This can be well understood by the fact that the high-energy possessed by the system allows the dynamics to not be constrained within the valley of the PES as the low-energy dynamics would. Therefore, the subtle difference between PESs is no longer critical at high energies.

To gain a better understanding of the coalescence mechanism, the AB + C reaction was further studied for each metal at the energies of 0.1 and 1.0 eV by varying the incident angle from 0° to 90° as discussed in section 2.2. These calculations were performed using the bulk and cluster PESs. The results are summarized in Table 4 for 1.0 eV and Table 5 for 0.1 eV.

Before discussing the coalescence mechanism, we summarize the sensitivity of reaction dynamics on the PES for different metals. The products for gold are quite varied between the two PESs. Pt and Ag are also more sensitive to the PES. At the lower energy of 0.1 eV, the MD results are

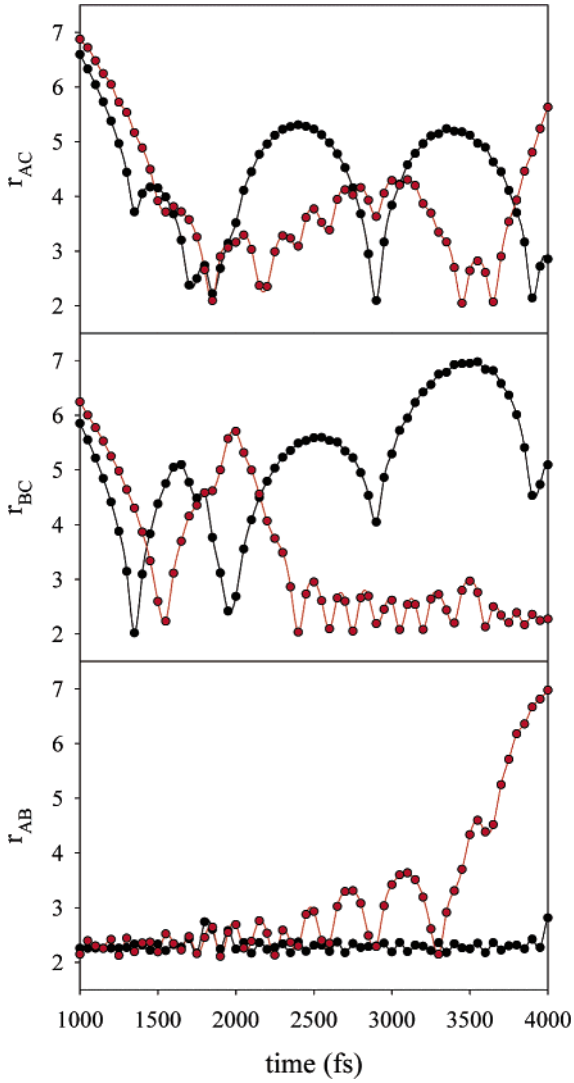

Figure 4. Interatomic distances (in Å) as a function of time (fs) for the products of the AB + C reaction of Pt atoms with initial kinetic energy of 0.1 eV and an incident angle of 75°. Results are shown for the bulk (black) and cluster (red) PESs for atoms (a) AC, (b) BC, and (c) AB.

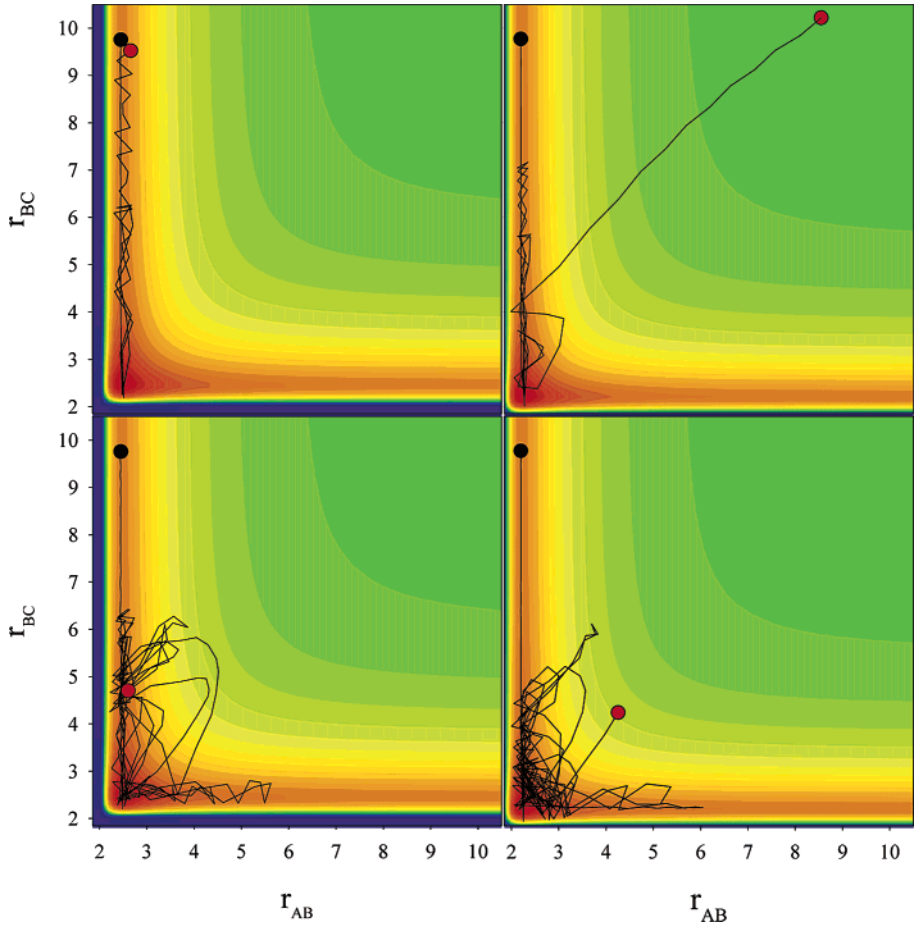

Figure 5. Trajectories (black curves) for the AB + C reaction of Ir atoms with initial kinetic energy of 1.0 eV (top figures) and 0.1 eV (bottom figures) obtained with the original bulk (left figures) and cluster optimized (right figures) PESs. The interatomic distances, r_{AB} and r_{BC}, are given in Å. The incident angle is 45° in all cases. The black and red circles indicate the starting and ending distances (in Å), respectively. The contour plots, which are the same as shown in Figure 3, serve as guidance only as they are the collinear case of the corresponding PESs on which these trajectories were obtained.

very sensitive to the PES, as shown in Table 5. Different products were obtained with the bulk and cluster PESs for all incident angles. In fact, the products are completely different for all metals at the incident angles of 30°, 45°, and 60°.

In order to further investigate the differences between the bulk and cluster PESs, the interatomic distances were plotted vs time for the case of Pt_2 + Pt with initial kinetic energy of 0.1 eV and an incident angle of 75°. The r_{AC}, r_{BC}, and r_{AB} distances are shown in Figure 4 (parts a−c, respectively) over the time of 1000−4000 fs. At the beginning of the calculation, very little difference is seen using the bulk and cluster PESs. However, as the time progresses, the differences become more pronounced. By 4000 fs, different products are formed with the different PESs.

Figure 5 shows the trajectories for the Ir_2 + Ir reaction with an incident angle of 75° and initial kinetic energy of 1.0 eV (top) and 0.1 eV (bottom) obtained with the original (left) and optimized (right) PESs. We note that the contour plots of PES illustrated in Figure 5 correspond to the collinear case. These contours are for guidance only as they are not the actual PESs that the trajectories were formed from. For 1.0 eV, the Sutton−Chen PES with original parameters predicts an AB dimer remains, while with the cluster parameters an AC dimer is formed. The difference between the left and right black curves in the top figures shows clearly that the trajectory that these atoms follow is impacted greatly by the PES. At the lower energy of 0.1 eV, a nearly triangular structure of Ir_3 is formed with the original PES, while a dimer is the product with the cluster parameters. In summary, the results discussed above demonstrate that the accuracy of PES is essential in order to obtain meaningful results for coalescence.

As in our discussion of the impact of kinetic energy to coalescence, here we confine our discussion of the incident angle effect to the MD results based on the cluster optimized PES, shown in Tables 4 and 5. At the higher energy of 1.0 eV (Table 4), the collision results in reactive scattering in all cases at the incident angles of 0° and 15°. As the incident angle is increased toward perpendicular, the collision becomes elastic in many cases. These results show that the incident angle plays a key role in the coalescence process.

At the lower energy of 0.1 eV (Table 5), the collision for Ir systems becomes increasingly more reactive and complex with the increase of incident angle. A trimer is still formed at the end of our simulation at incident angles of 30° and 45°. Many Au trimers were also still formed at the end of MD simulations. These results further illustrated that coalescence mechanism is very different at low kinetic energies for different metals, while it is less so at high kinetic energies.

Finally, we mention the effect of metal on the coalescence. The results in Tables 3−5 have shown that more similarities exist between Ir and Ag and between Pt and Au. This may be due to the similarities of the Sutton−Chen parameters between Ir and Ag and between Pt and Au.

4. Conclusions

We compared the binding energy obtained from the original Sutton−Chen potential to our DFT results for the dimers, trimers, and 8- and 13-atom clusters of iridium, platinum, gold, and silver. It was found that the original Sutton−Chen potential was not accurate for describing small metal clusters. This can be understood by the fact that the Sutton−Chen potential parameters were optimized to the bulk properties for each of the metals studied. In this work, we optimized these parameters to our DFT results for the small clusters and constructed a new PES for each metal.

Molecular dynamics simulations were performed using the bulk and cluster PESs to study the coalescence of a 3-atom system, AB + C. The reaction AB + C was investigated with various incident angles and initial kinetic energy. The MD results demonstrated that the accuracy of a PES is critical to the outcome of the dynamics simulations, especially at lower energies, for all four metals. The MD results also show that the products of coalescence were greatly impacted by both the incident angle and the energy. The choice of metal will also influence the outcome of coalescence, though more similarities were observed between Ir and Ag and between Pt and Au.

Acknowledgment. We gratefully acknowledge the support from the American Chemical Society Petroleum Research Fund under Grant No. 41572-G5 and the Materials Technology Center of Southern Illinois University at Carbondale.

References

(1) Campbell, C. T.; Parker, S. C.; Starr, D. E. *Science* **2002**, *298*, 811.

(2) Baletto, F.; Ferrando, R. *Rev. Mod. Phys.* **2005**, *77*, 371.

(3) Lisiecki, I. *J. Phys. Chem. B* **2005**, *109*, 12231.

(4) Sanchez, A.; Abbet, S.; Heiz, U.; Schneider, W.-D.; Hakkinen, H.; Barnett, R. U.; Landman, U. *J. Phys. Chem. A* **1999**, *103*, 9583.

(5) Mason, T. G. Lin, M. Y. *J. Chem. Phys.* **2003**, *119*, 565.

(6) Mitchell, C. E. J.; Howard, A.; Carney, M.; Egdell, R. G. *Surf. Sci.* **2001**, *490*, 196.

(7) Xu, L. J.; Henkelman, G.; Campbell, C. T.; Jonsson, H. *Phys. Rev. Lett.* **2005**, *95*, 146103.

(8) Zhu, H. H.; Lu, L.; Fuh, J. Y. H. *J. Mater. Process. Technol.* **2003**, *140*, 314.

(9) Zhang, Y. M.; Chen, Y. W.; Li, P. J.; Male, A. T. *J. Mater. Process. Technol.* **2003**, *135*, 347.

(10) Teixeira, A.; Giudici, R. In *Catalyst Deactivation 2001, Proceedings*; 2001; Vol. 139, p 495.

(11) Smejkal, Q.; Linke, D.; Bentrup, U.; Pohl, M. M.; Berndt, H.; Baerns, M.; Bruckner, A. *Appl. Catal,. A* **2004**, *268*, 67.

(12) Tang, Y.; Loh, H. T.; Wong, Y. S.; Fuh, J. Y. H.; Lu, L.; Wang, X. *J. Mater. Process. Technol.* **2003**, *140*, 368.

(13) Santra, A. K.; Goodman, D. W. *J. Phys.: Condens. Matter* **2003**, *15*, R31.

(14) Ojeda, M.; Rojas, S.; Garcia-Garcia, F. J.; Granados, M. L.; Terreros, P.; Fierro, J. L. G. *Catal. Commun.* **2004**, *5*, 703.

(15) Minay, E. J.; Boccaccini, A. R.; Veronesi, P.; Cannillo, V.; Leonelli, C. *Adv. Appl. Ceram.* **2005**, *104*, 49.

(16) Kwon, Y. S.; Dudina, D. V.; Korchagin, M. A.; Lomovsky, O. I. *J. Mater. Sci.* **2004**, *39*, 5325.

(17) Kim, B. K.; Ha, G. H.; Lee, D. W. *J. Mater. Process. Technol.* **1997**, *63*, 317.

(18) Hsieh, Y. Z.; Chen, J. F.; Lin, S. T. *J. Mater. Sci.* **2000**, *35*, 5383.

(19) Greco, A.; Licciulli, A.; Maffezzoli, A. *J. Mater. Sci.* **2001**, *36*, 99.

(20) Heinrichs, B.; Noville, F.; Pirard, J. P. *J. Catal.* **1997**, *170*, 366.

(21) Duck, J.; Niebling, F.; Neesse, T.; Otto, A. *Powder Technol.* **2004**, *145*, 62.

(22) Barbero, J.; Pena, M. A.; Campos-Martin, J. M.; Fierro, J. L. G.; Arias, P. L. *Catal. Lett.* **2003**, *87*, 211.

(23) Banhart, J. *Prog. Mater. Sci.* **2001**, *46*, 559.

(24) Kwon, Y. S.; Savitskii, A. *J. Mater. Synth. Process.* **2001**, *9*, 299.

(25) Tian, D.-X.; Guo, X.-Y. *Comput. Mater. Sci.* **2005**, *34*, 14.

(26) Hendy, S.; Brown, S. A.; Hyslop, M. *Phys. Rev. B* **2003**, *68*, 241403.

(27) Finnis, M. W.; Sinclair, J. E. *Philos. Mag. A* **1984**, *50*, 45.

(28) Daw, M. S.; Baskes, M. I. *Phys. Rev. B* **1984**, *29*, 1285.

(29) Mrovec, M.; Nguyen-Manh, D.; Pettifor, D. G.; Vitek, V. *Phys. Rev. B* **2004**, *69*, 094115.

(30) Murrell, J. N.; Mottram, R. E. *Mol. Phys.* **1990**, *62*, 571.

(31) Sutton, A. P.; Chen, J. *Philos. Mag. Lett.* **1990**, *64*, 139.

(32) Doye, P. K.; Wales, D. J. *New J. Chem.* **1998**, 733.

(33) Pawluk, T.; Hirata, Y.; Wang, L. *J. Phys. Chem. B* **2005**, *109*, 20817.

(34) Xiao, L.; Wang, L. *J. Phys. Chem. A* **2004**, *108*, 8605.

(35) Xiao, L.; Wang, L. *Chem. Phys. Lett.* **2004**, *392*, 452. Xiao, L.; Tollberg, B.; Hu, X.; Wang, L. *J. Chem. Phys.* **2006**, *124*, 114309.

(36) Yukna, J.; Tang, H.; Wang, L. *J. Chem. Phys.* Submitted for publication.

(37) Press, W. H.; Flannery, B. P.; Teukolsky, S. A.; Vetterling, W. T. *Numerical Recipes [Fortran Version]*; Cambridge University Press: 1990.

(38) Miedema, A. R.; Gingerich, K. A. *J. Phys. B: At., Mol. Opt. Phys.* **1979**, *12*, 2081.

(39) Taylor, S.; Lemire, G. W.; Hamrick, Y. M.; Fu, Z.; Morse, M. D. *J. Chem. Phys.* **1988**, *89*, 5517.

(40) Gupta, S. K.; Nappi, B. M.; Gingerich, K. A. *Inorg. Chem.* **1981**, *20*, 966.

(41) Bishea, G. A.; Morse, M. D. *J. Chem. Phys.* **1991**, *95*, 5646.

(42) Morse, M. D. *Chem. Rev.* **1986**, *86*, 1049.

CT600257P